Interleukin 22 ameliorates neuropathology and protects from central nervous system autoimmunity

Mary J. Mattapallil, Jennifer L. Kielczewski[1], Carlos R. Zárate-Bladés[2], Anthony J. St Leger[3], Kumarkrishna Raychaudhuri[4], Phyllis B. Silver, Yingyos Jittayasothorn, Chi-Chao Chan, Rachel R. Caspi[*]

Laboratory of Immunology, National Eye Institute, National Institutes of Health, Bethesda, MD, 20892, USA

ABSTRACT

IL-22 has opposing effects in different tissues, from pro-inflammatory (skin, joints) to protective (liver, intestine) but little is known about its effects on neuroinflammation. We examined the effect of IL-22 on retinal tissue by using the model of experimental autoimmune uveitis (EAU) in IL-22$^{-/-}$ mice, as well as by intraocular injections of recombinant IL-22 or anti-IL-22 antibodies in wild type animals. During EAU, IL-22 was produced in the eye by CD4$^+$ eye-infiltrating T cells. EAU-challenged IL-22$^{-/-}$ mice, as well as WT mice treated systemically or intraocularly with anti-IL-22 antibodies during the expression phase of disease, developed exacerbated retinal damage. Furthermore, IL-22$^{-/-}$ mice were more susceptible than WT controls to glutamate-induced neurotoxicity, whereas local IL-22 supplementation was protective, suggesting direct or indirect neuroprotective effects. Mechanistic studies revealed that retinal glial Müller cells express IL-22rα1 *in vivo*, and *in vitro* IL-22 enhanced their ability to suppress proliferation of effector T cells. Finally, IL-22 injected into the eye concurrently with IL-1, inhibited the (IL-1-induced) expression of multiple proinflammatory and proapoptotic genes in retinal tissue. These findings suggest that IL-22 can function locally within the retina to reduce inflammatory damage and provide neuroprotection by affecting multiple molecular and cellular pathways.

1. Introduction

IL-22 is produced by cells of the immune system and acts on non-hematopoietic cells by modulating tissue responses during inflammation [reviewed in 1, 2]. IL-22 is produced by innate as well as adaptive immune cells. Th17 cells are a major source of IL-22, but the cytokine is also produced by Th1 cells as well as by innate NK, NKT and γδ T cells, as well as by group 3 innate lymphoid cells (ILC3) and lymphoid tissue inducer cells (LTi). The effects of IL-22 are largely directed at tissue cells that express functional heterodimeric IL-22 receptor that is composed of the Il-10r2 chain, shared with other members of the Il-10 family, and the unique IL-22rα1 chain. Cells expressing IL-22 receptor include epithelial cells of the skin, intestine, and lung and the acinar cells of the pancreas, liver, and kidney [3,4]. In animal models, effects of IL-22 on the tissue are diverse and often contradictory, ranging from pro-inflammatory (psoriasis, bleomycin-induced airway disease, sepsis-induced kidney damage, autoimmune arthritis) to protective (hepatitis, bacterial intestinal and lung infections, atopic lung fibrosis) [1,2].

Autoimmune uveitis (also known as uveoretinitis), is a sight threatening inflammation of the light-sensitive tissues of the eye. Each year about 150,000 new cases of autoimmune uveitis are reported in the US alone; autoimmune uveitic diseases are estimated to account for 10–15% of severe visual handicap in the western world [5]. The disease is often associated with memory T cell responses to retinal antigens and elevated Th1 and Th17 cytokines [6,7]. Human autoimmune uveitis has an experimental counterpart, known as experimental autoimmune

---

uveitis (EAU). EAU is induced in mice by immunization with the retinal protein IRBP in complete Freund's adjuvant [6]. In this model, retina specific Th1 as well as Th17 cells are induced and both are involved in pathology [8].

The role of IL-22 in uveitis is controversial. Although PBMC from uveitis patients [9] as well as T cell clones generated from ocular samples of patients with Behcet's disease produced IL-22 [10], a causal link to disease is unclear and conflicting results were reported regarding the effect of IL-22 on ocular cells. While Li et al. [9] reported that cultured human retinal pigment epithelial (RPE) cells treated with IL-22 showed apoptotic changes, Kim et al. [11] demonstrated the opposite using ARPE19 cells, a human RPE cell line widely used to study RPE cell responses. Similarly to humans [10], IL-22 is also produced by T cells in uveitic mouse eyes [8,10], but whether it has pathogenic or protective effects is not clear and it is unknown which ocular cells express the IL-22 receptor. Systemic administration of recombinant IL-22 was reported to ameliorate EAU through tolerogenic effects on DC and enhancement of T-reg cells [12], but such systemic effects on the immune response do not address tissue-specific effects of IL-22.

CNS autoimmunity results in deterioration of end organ function due to damage to neural tissues driven by a complex interaction between immune and local cellular elements. In the eye, an inflammatory environment stimulates resident cells like glial Muller cells, astrocytes, and microglia to produce mediators that can either damage or protect the neural tissue. The objective of this study was to understand the effect of IL-22 on ocular tissue during autoimmune uveitis and to examine its role in modulation of disease severity. Our data suggest that IL-22 may have immunomodulatory and neuroprotective effects in the eye and that this protection may be connected to its effects on retinal glial Muller cells.

In-vitro results from our study suggest that one of the mechanisms of IL-22 mediated amelioration of ocular inflammation could be enhanced suppression of T cells by resident Muller cells. Ingenuity pathway analysis based on the genes expressed in the retina during inflammation suggests that IL-22 modulates several functional pathways, including downregulation of T cell differentiation, downregulation of apoptosis of ganglion cells, downregulation antibody dependent cell-mediated cytotoxicity, upregulation of new DNA synthesis and upregulation of leukocyte emigration from ocular tissue. IL-22 stimulated Müller cells expressed neuroprotective factors and in a live animal model of chemically induced neurodegeneration, presence of IL-22 increased the survivability of retinal ganglion cells (RGCs). These data are compatible with an immunoregulatory and neuroprotective role of IL-22 in the eye.

2. Materials and methods

2.1. Animals

IL-22 knockout (KO) mice on C57BL/6 background were generated by Genentech and have been described previously [13]. Inbred mouse strains C57BL/6J and B10.RIII were obtained from Jackson Laboratories. The animals were maintained under specific-pathogen-free conditions at NIH animal facility on standard chow and water ad libitum. Wild-type littermates (WT LTM) of each KO strains were bred homozygously from the earlier crosses and served as controls in the experiments. Animal care and use conformed to Institutional guidelines. All experiments were conducted under an institutionally approved animal study protocol (ASP# NEI-581).

2.2. Induction, treatment, and evaluation of EAU

Uveitogenic peptides for C57BL/6 (peptide IRBP1-20 GPTHLFQPS-LVLDMAKVLLD), and B10.RIII strain (peptide IRBP161-180 SGIPYIIS-YLHPGNTILHVD) were synthesized by AnaSpec (Fremont, CA) using solid-state methodology and was used at 80% purity. Bovine IRBP

protein was purified by ConA sepharose affinity chromatography and FPLC [14]. Strains on C57BL/6 background were actively immunized subcutaneously with 150 μg bovine IRBP and 300 μg human peptide IRBP1-20 emulsified 1:1 v/v in complete Freund's adjuvant containing 2.5 mg/ml *Mycobacterium tuberculosis* H37RA (Difco, Detroit, MI). A total of 200 μl of emulsion was distributed to three sites, base of the tail (100 μl) and the hind legs (50 μl each). Mice also received a single dose of 0.5 μg pertussis toxin (Sigma-Aldrich, St. Louis, MO; Cat# P7208) in 100 μl of 1x PBS intraperitoneally on the same day of immunization. For induction of EAU in B10.RIII mice by adoptive transfer 1–2 million freshly stimulated cells from an uveitogenic T cell line specific to IRBP peptide 161–180 [15] were used. Cells stimulated with peptide 161–180 (1.0 μg/ml) for 48 h were suspended in medium plus 2% mouse serum and were injected intraperitoneally into naive syngeneic recipients. For systemic treatment, experimental animals were given 500 μg of anti-mouse IL-22 antibody (clone 8E11, obtained from Genentech) or its isotype control (clone MOPC-21, BioXcell) intraperitoneally on days 7, 9, 11, 13, and 15 post-immunization. For local treatment, animals were given 7 μg/2 μl/eye anti-mouse IL-22 antibody or isotype on day 8 post-immunization as a single bilateral intravitreal injection.

Eyes were examined at regular intervals using a binocular microscope to assess severity of the lesions. Experiments were terminated on day 21 post-immunization for tissue collection. Eyes were collected and fixed with 4% Glutaraldehyde (Fisher Scientific) in 1X PBS for 1 h followed by 10% neutral formaldehyde (Sigma-Aldrich) in PBS for 24 h before grossing and embedding. Methacrylate blocks were cut into 6 μm sections and stained with H&E for histological analysis. Sections were evaluated by an independent observer (CCC) and were scored on a scale of 0 (no disease) to 4 (very severe disease) in half-point increments, according to the number and size of lesions, using a semi-quantitative scale described previously [16].

2.3. Induction and evaluation of EAE

MOG$_{35-55}$ peptide (MEVGWYRSPFSRVVHLYRNGK) was purchased from AnaSpec, Inc. CA (Cat# 60130). Mice were immunized by subcutaneous injection of 200 μg MOG$_{35-55}$ peptide emulsified 1:1 v/v in CFA containing 5.0 mg/ml M. *tuberculosis*. Mice also received two doses of 0.25 μg Pertussis Toxin in 100 μl of 1x PBS intraperitoneally on day 0 and day 2 of immunization. Clinical evaluation of EAE symptoms was described previously [17]. Briefly, mice were scored daily starting day 8 post-immunization as follows: 0, no detectable signs of EAE; 0.5, distal limp tail; 1, complete limp tail; 1.5, limp tail and weakness of hind limbs; 2, unilateral partial hind limb paralysis; 2.5, bilateral partial hind limb paralysis; 3, complete bilateral hind limb paralysis; 3.5, complete hind limb paralysis and unilateral fore limb paralysis; 4.0, total paralysis of fore and hind limbs, rapid breathing and recumbency (score 4 to be killed); 5, death.

2.4. Induction of glutamate toxicity to retinal ganglion cells (RGCs) and evaluation of RGC survival

Retinal ganglion cells (RGCs) of mice were labeled with fluorogold dye, before induction of glutamate toxicity, for tracing live neuronal cells by retrograde uptake. Briefly, C57BL/6J or IL-22 KO mice or wild type littermates were anesthetized and an opening was made on the cranium (2.92 mm posterior to bregma, 0.5 mm lateral to the midline, and at a depth of 2 mm from the skull) above the superior colliculi of each side of brain. With the use of a stereotactic device and a Hamilton injector syringe, mice were injected with 1 μl of 4% Fluorogold (Fluorochrome, Denver, CO) solution in saline. After completion of the injection, skin on the scalp was sutured and animals were allowed to recover for one week to allow for adequate labeling of RGCs. Neurotoxicity was induced in fluorogold labeled mice by intravitreal injection of 1 μl of 400 nM solution of L-glutamate (Sigma-Aldrich, St.

Louis, MO) dissolved in PBS with or without 1 μl of recombinant mouse IL-22 (Peprotech, Rocky Hill, NJ) at a concentration of 200 ng/μl dissolved in PBS in one eye and 2 μl of PBS in the contralateral eye which served as an internal control for each mouse. Mice were euthanized one week after glutamate challenge and their eyes were evaluated for loss of RGCs. Survival of RGCs was assessed as follows. Enucleated eyes were fixed in 4% paraformaldehyde in PBS for 2 h. Retinas were detached and prepared as flattened whole mounts on glass slides for imaging. Labeled cells from 15 fields of identical size were imaged using a confocal microscope (Olympus FV1000) and counted using Image J software at $40\times$ magnification. The counted fields were located approximately the same distance from the optic disc (0.3 mm) to eliminate variations in RGC density as a function of distance from the optic disc. Average number of RGCs per field in each retina was calculated for each retina. Number of RGCs in the contralateral (uninjured) eye was also counted and served as an internal control.

2.5. Cell culture and proliferation assays

Single cell suspensions of lymphocytes from draining LN were collected and cultured *in vitro* in the presence of increasing doses (0.2 μg/ml, 2.0 μg/ml, and 20.0 μg/ml) of IRBP protein in HL-1 medium (Lonza, Walkersville, Inc.) with additives and α-MMP (100 mg/ml) to neutralize the effect of contaminating Con-A in IRBP preparation. Cells were incubated at 37 °C and 5% CO_2 for a total of 72 h with H^3 pulsing during the last 18 h of incubation. Level of H^3 incorporation was measured using scintillation counting. For cytokine assays cells were cultured with 20 μg/ml IRBP protein and culture supernatants were collected after 48 h of incubation.

Mouse Müller cells were isolated from eyes of adult mice and were cultured as monolayers in presence of 10% Concanavalin A stimulated spleen cell supernatant as described previously [18]. Prior to use in experiments, Müller cells were plated in slide chambers or in 96-well plates and allowed to adhere overnight (approximately 18 h). For T cell suppression assay, Muller cells were cultured with (500 ng/ml) or without murine rIL-22 for three days, irradiated (3000 rads), plated in 96-well plate at a concentration of 1×10^4 cells/well, and allowed to adhere for 18 h. On the day of the assay, freshly isolated splenic cells from naïve C57BL/6J mice were enriched for T cells using murine T cell enrichment column (R&D systems, MN) and were labeled with proliferation dye eF670 (eBioscience, CA). Dye labeled T cells $(1 \times 10^5$ cells/well) were co-cultured with or without irradiated Muller cells in the presence or absence of anti-CD3 (1 μg/ml), anti-CD28 (0.5 μg/ml), and murine rIL-22 (500 ng/ml, PeproTech) for 72 h at 37 °C and 5% CO_2. Inhibition of T cell proliferation was quantified by FACS analysis using the Proliferation tool in FlowJo software (Tree Star Inc., OR).

2.6. Analysis of cytokines and infiltrating cells from eyes of EAU mice

Enucleated eyes were collected into HL-1 medium containing 1 mg/ml collagenase D (Roche Life science). External tissues (optic nerve and connective tissues) were trimmed and the globes were transferred into 1 ml serum free HL-1 medium (10 eyes from 5 mice per group) or two eyes of individual mouse in 100 μl PBS (for measuring Tgfβ) containing Halt protease inhibitor cocktail (Thermo Fisher Scientific). After carefully removing the lens by dissection along the limbus, the tissue was minced with scissors, dispersed by vigorous trituration, and centrifuged. The clarified supernatant was collected for cytokine analysis. The pellet was resuspended in 3 ml HL-1 medium containing 10% FCS, and 1 mg/ml collagenase D and incubated for 1 h in 37 °C. The cells were dispersed by trituration using a transfer pipette, washed, filtered through 40 μm strainer, and suspended in 3 ml RPMI medium containing 10% fetal calf serum for counting. Cells were incubated $(4 \times 10^6$ cells/3 ml/well of 24 well plate) with or without PMA/ionomycin and monensin and stained for intracellular cytokine analysis and

immunophenotyping by FACS, as described below. Non-inflamed eyes from unimmunized donors did not yield sufficient leukocytes for analysis.

2.7. Cytokine measurement in culture supernatants or eye extracts

IL-22 in culture supernatants and eye extracts was quantitated using mouse-IL-22 Duoset ELISA development system (catalog # DY582, R&D systems, MN). Multiplex cytokine analysis was done using SearchLight Assay service (Aushon Biosystems, Billerica, MA) or the BioPlex Pro™ Mouse Cytokine assay kit (Bio-Rad Lab, Inc. Hercules, CA) and their Luminex-based system (Bio-Rad Lab, Inc. Hercules, CA). Data from the BioPlex assay were analyzed using BioPlex manager software v6.1 (Bio-Rad Lab, Inc. Hercules, CA). Tgfβ1 in eye extracts was measured using Mouse Tgf beta 1 ELISA kit (Invitrogen – catalog# BMS608-4) per manufacturer's instructions. Data were normalized to cytokine levels in medium or PBS alone (for eye extract) or in cell culture supernatants without antigenic stimulation.

2.8. Intra-cellular cytokine staining for FACS

Intracellular cytokine staining was done after stimulating one million cells with phorbol 12-myristate 13-acetate (PMA 10 ng/ml) and ionomycin (0.5 μg/ml) and Monensin (BD GolgiStop™, BD Bioscience) for 5–6 h at 37 °C. Cells were fixed (4% paraformaldehyde) and permeabilized (0.5% Triton-X and 0.1% BSA) before staining with antibodies. Mouse anti-IL-22 antibody (clone 3F11.3 from Genentech) was conjugated with AF647 dye (catalog# A-20186, Molecular Probes, Eugene, OR) according to manufacturer's instructions and was used at dilution of 1:2000. Anti-mouse antibodies such as anti-Il-17A (clone TC11-18H10), anti-IFNγ (clone XMG1.2), anti-CD8α (clone 53-6.7), anti-TCRβ (clone H57-957), anti-CD45 (clone 30-F11) and anti-γδ TCR (clone GL3) were purchased from BioLegend, San Diego, CA.; anti-CD4 (Clone GK15), anti-IL-10 (clone JES5-16E3), and anti-Foxp3 (clone FJK-16s) were purchased from eBioscience, San Diego, CA. Mouse CD1d Tetramer (APC, PE, or AF488) was obtained from the NIH Tetramer Core Facility at Emory University, GA.

2.9. Immunohistochemistry and confocal imaging

Following enucleation, eyes were fixed in paraformaldehyde 4% for 4 h. Eyecups were separated under a dissecting microscope removing the tissue around the sclera. The samples were washed in 1X PBS and immediately immersed in 7% agarose to form blocks for vibratome sectioning. Sections of 100 μm thickness were obtained, avoiding dehydration of the sample. The samples were then washed in 1X PBS and blocked with 10% FBS in immunocytochemistry (ICC) buffer (0.5% BSA, 0.2% Tween 20, 0.05% sodium azide) for 4 h. The samples were incubated with primary antibodies in ICC buffer overnight. After three washes with ICC buffer for 15 min each, the samples were incubated with secondary antibodies for 2 h in ICC buffer containing Hoechst 33342 (Pierce Biotechnology, Rockford, IL) 1:1000 dilution. Samples were rinsed and mounted in FluorSave reagent (Calbiochem) for confocal microscopy. The following antibodies were used: Rabbit anti-IL-22Rα polyclonal antibody (catalog# ab5984, Abcam) was used at a dilution of 1:200 along with the secondary antibody goat anti-rabbit-IgG Alexa Fluor 488 (catalog# A11008, Molecular Probes) or goat anti rabbit-Alexa 555 (catalog# A21428, Molecular probes) at a dilution of 1:500; rat anti-GFAP monoclonal antibody (catalog#13–0300, Molecular Probes) was used at a dilution of 1:500 with the secondary antibody anti rat-IgG-Alexa Fluor 555 (catalog# 4417-S, Cell Signaling) was used at a dilution of 1:500 or chicken anti GFAP polyclonal antibody (catalog# AB541, Millipore) was used at a dilution of 1:200 with the secondary antibody Goat anti chicken-Alexa 488 (catalog# A11309, Molecular probes) was used at a dilution of 1:300. Mouse Müller cells from primary cultures maintained as described previously [18] were

plated in a Lab-Tek Permanox chamber slide (Thermo Scientific) at a concentration of 1×10^4 cells per chamber and cultured overnight before staining.

Images were obtained using 20x and $40\times$ objectives of a scanning Zeiss LSM 702 Confocal Microscope (Carl Zeiss Microimaging Inc., Thornwood, NY.). The samples were scanned using the tile scan feature and Z-stack function of the Zen Blue software (Carl Zeiss Microimaging GmbH, Jena, Germany). Multiple z-series images were collected at 1084×1084 pixel resolution at a depth of 8 bits per channel, voxel dimensions of 0.621×0.621 x 0.62 for the x,y,z-axis. Maximal intensity projection images are present in the figures.

2.10. Gene expression profiling and pathway analysis of the transcriptome

Retinal tissues were isolated as described before [19,20] from mouse eyes injected intravitreally with PBS (2 μl/eye) or Il-1α (100 ng in 2 μl/eye) or IL-22 (200 ng in 2 μl/eye) or Il-1α + IL-22, 24 h after injection. Total RNA was isolated using RNeasy Mini kit (Qiagen Inc., Valencia, CA) and cDNA was synthesized using oligo-dT and SuperScript III reverse transcriptase as per manufacturer's instruction (Life Technologies, Grand Island, NY). Gene expression profiles of 48 genes as custom Taqman Array plates (Life Technologies, Grand Island, NY, see Supplementary Table 1 for Taqman probe assay ID) or expression of individual genes using Taqman assays (see Table 1) was measured on Applied Biosystems 7500 Fast system (Life Technologies, Grand Island, NY) by real time qRT-PCR method. Data were analyzed by Comparative C_T ($\Delta\Delta C_T$) method using ABI 7500 software v2.0.6 (Life Tech. Corp. Carlsbad, CA). Relative Quantitation of gene transcripts was measured after normalization of each sample to its own expression of *Gapdh* or β-Actin gene (endogenous control) and samples were compared between each other after normalization to PBS injected sample or untreated Muller cells as reference sample. Heat map was generated by DataAssist v3.0 software (Life technologies, CA). Functional analysis of the transcriptome profile and molecular networks were generated through the use of QIAGEN's Ingenuity Pathway Analysis (IPA®, QIAGEN Redwood City, www.qiagen.com/ingenuity) by uploading fold change expression values obtained from Taqman assay. Ingenuity Pathway Analysis (IPA) uses bibliographic database (knowledge base) to classify the genes implicated in each function. IPA uses Fischer's exact test to calculate p-values to determine the probability that each biological function assigned to that data set is due to chance alone.

Table 1
IL-22 treatment enhanced expression of anti-inflammatory and neuroprotective genes in Muller cells.

Genes (*Mus musculus*)	Taqman Assay ID	Fold change
β-Actin	Mm02619580_g1	1.00
A2m	Mm00558642_m1	0.96
Bdnf	Mm04230607_s1	1.41
Cd274 (Pdl1)	Mm00452054_m1	1.57
Gapdh	Cat# 4352932	1.83
Gdnf	**Mm00599849_m1**	**2.28******
Hif1α	Mm00468869_m1	1.64
Il-10rβ	Mm00434157_m1	1.84
Il-19	**Mm01288324_m1**	**2.56*****
Lag3	Mm00493071_m1	1.98
Ngf	**Mm00443039_m1**	**2.22***
Stat3	Mm01219775_m1	1.47
Tgfβ1	Mm00441724_m1	1.43
Tgfβ2	Mm00436955_m1	1.36
Tgfβ3	Mm00436960_m1	1.35
Thbs1	Mm00449032_g1	1.98
Thbs2	**Mm01279240_m1**	**2.45****
Vegfα	Mm00437306_m1	1.76

*Asterisks denote 'p' values, tested using Welch's 't' test for unpaired parametric values with unequal standard error. The number of asterisks shows the level of significance, from < 0.01 to < 0.00001.

2.11. Western blotting

Muller cells were deprived of spleen conditioned medium for 48 h in culture medium (DMEM with 10% FBS) and then pulsed with IL-22 (500 ng/ml) or without any treatment (control) for 45 min. Adherent Muller cells were rinsed with PBS in the plate and cell lysates were prepared in SDS lysis buffer supplemented with protease inhibitors (leupeptin - 10 μg/ml, aprotinin - 20 μg/ml, PMSF - 1 mM, Sodium fluoride - 50 mM, Sodium ortho vanadate - 1 mM, EDTA - 1 mM). Equal amounts of protein lysates from control and IL-22 treated samples were run on denaturing SDS PAGE followed by transfer to nitrocellulose membrane. Blots were probed with primary antibodies against pSTAT3 (Cell Signaling, cat# 9131), STAT3 (Cell Signaling, cat# 12640), pP38 MAPK (Cell Signaling, cat# 4511) and P38 MAPK (Cell Signaling, cat# 8690). HRP conjugated anti rabbit secondary antibodies (ThermoFisher Scientific, cat# 31460) and SuperSignal West Pico chemiluminescent substrate (ThermoFisher Scientific, cat# 34580) were used for detection according to manufacturer's protocol.

2.12. Statistical analysis

Statistical differences between groups were analyzed using GraphPad Prism 6.0d software as follows: for comparison of EAU scores between strains non-parametric *t*-test (Mann-Whitney U method) and for comparison of EAE scores between strains during the course of disease two-way ANOVA were used; differences between groups for lymphocyte proliferation assay were analyzed by two-way ANOVA or by two-tailed unpaired 't' test; Loss of RGCs was analyzed using one way ANOVA or Welch's unpaired 't' test; Experiments were repeated at least twice with identical results, and usually three or more times. Representative experiments or pooled data are shown, as specified.

3. Results

3.1. IL-22 production is elevated during the adaptive phase of experimental autoimmune uveitis

A recent report showed increased levels of IL-22 message in the PBMCs of uveitis patients [9]. We were therefore interested in looking at IL-22 production during various stages of EAU. C57BL/6J mice were immunized for EAU with IRBP and their draining lymph node and spleen cells were stimulated *in vitro* with the immunizing antigen. Antigen-induced levels of IL-22 in supernatants of these cultures peaked around day 9 post-immunization (Fig. 1A), which is just prior to clinical disease onset that typically occurs between days 10 and 12. Cells infiltrating the eyes were isolated at various time points and immediately phenotyped for production of IL-17 and IL-22 by intracellular cytokine staining after a PMA/Ionomycin pulse. A high frequency of IL-17 + lymphocytes was found in the eye on day 14 (peak of disease). IL-22 production was present in IL-17-positive and, to a lesser extent, also in IL-17-negative eye-infiltrating lymphocytes (Fig. 1B). Major producers of this cytokine in the ocular environment were αβ T cells (Fig. 1C) with negligible or no contribution from γδ T cells or NK T cells (data not shown).

3.2. Genetic deficiency of IL-22 in mice exacerbates pathology in the CNS

If presence of IL-22 in the inflamed eye has a protective effect, then lack of IL-22 should result in development of more severe disease. Indeed, mice genetically deficient in IL-22 protein when immunized for EAU developed a more severe form of uveitis than their WT littermate controls (Fig. 2A). There was increase in thickness of the retinal layers due to inflammation, serous detachment and extensive damage to neuroretina in the IL-22 KO mice when compared to their WT littermates (Fig. 2B). There was no apparent difference in the composition of inflammatory infiltrate recruited into the eyes, which consisted mainly
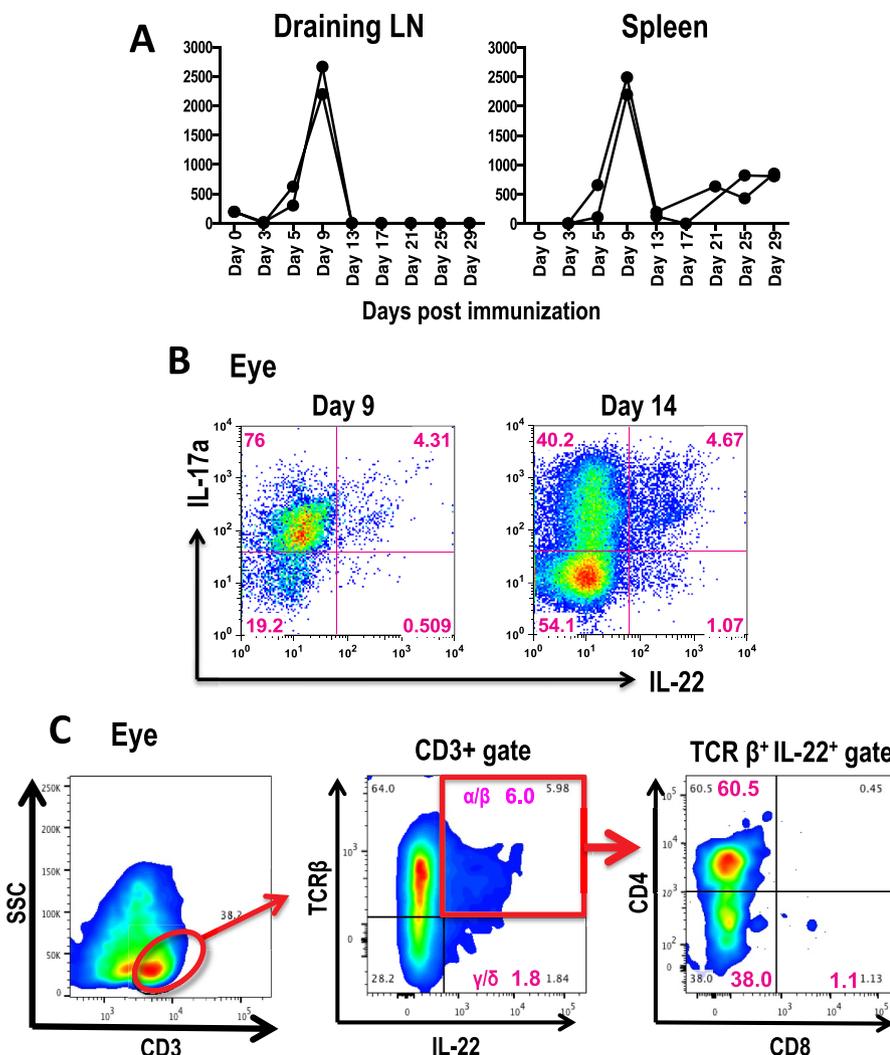
Fig. 1. IL-22 is produced both systemically and locally in the eye during Experimental Autoimmune Uveitis. (A) Level of IL-22 production by antigen induced T cells peaks at day 9 post immunization. Lymphocytes from draining lymph nodes (site of immunization) or spleen of C57BL/6J mice immunized with IRBP and its peptide IRBP1-20 were cultured with IRBP (10μg/ml) for 48 h and the amount of IL-22 production was measured (pg/ml) in the culture supernatants. Data shown is from two individual mice from a single representative experiment at each time point during the course of disease. The same trend was noticed in a second experiment. (B) Lymphocytes infiltrating uveitic eyes produce high levels of IL-22 during EAU. Cells from uveitic eyes (day 9 and day 14 post immunization) were stimulated ex-vivo with PMA/Ionomycin for 4 h and stained for intracellular cytokines. Staining of IL-22 and Il-17 positive cells (CD4$^+$ lymphocytes), in one representative mouse out of three mice per time point are shown. (C) Major source of IL-22 in uveitic eyes was from CD3$^+$TCRβ$^+$ T cells. On day 14 post-immunization eye infiltrating cells were collected from 2 to 3 C57BL/6J mice and were processed and stimulated as in Fig. 1B and stained with anti-CD3, anti-CD4, anti-CD8, anti-TCRβ, anti-TCRγδ, and anti-IL-22 antibodies. Staining of IL-22 in CD3$^+$ TCRβ$^+$ T cells in one representative mouse out of three mice are shown.

of mononuclear cells (not shown).

When lymphocytes from draining lymph nodes of mice immunized for EAU were stimulated in culture with the immunizing antigen there was significantly increased lymphocyte proliferative response in IL-22 knockout mice compared to WT littermates (Fig. 2C). Lymphocytes from IL-22 knockout mice also showed a trend towards increase in pro-inflammatory cytokine levels such as IL-6, IL-12p70, IFN-γ and TNF-α in response to immunizing antigen IRBP (Fig. 2D). We did not observe any differences in the production of IL-4, IL-5, IL-10 and IL-17A as a result of IL-22 deficiency (data not shown).

EAE is another autoimmune disease affecting neural tissue and is a widely used animal model for multiple sclerosis, where Th17 cells play a crucial role in the disease pathogenesis. Although IL-17 is the signature cytokine of Th17 cells, other cytokines of the pathway, including IL-21 and IL-22, could also play a role in the pathogenesis. Earlier reports showed that both IL-21 and IL-21 receptor has a protective role in EAE development [21,22]. However, the role of IL-22 in the pathogenesis of EAE is unclear [23,24]. Since EAU and EAE are two mechanistically similar disease models of autoimmune diseases affecting the CNS, we examined the effect of IL-22 in EAE development using IL-22 KO mice. As in the EAU model, IL-22 deficiency consistently resulted in enhanced disease scores (Fig. 2E), indicating that IL-22 can be protective in the CNS in general.

3.3. Systemic and local neutralization of IL-22 enhances EAU severity

IL-22 production by infiltrating lymphocytes was present in the eyes of EAU mice (Fig. 1) and was reported in Behcet's disease patients [10]. Systemically, increased expression of IL-22 transcripts was reported in PBMCs of patients with idiopathic uveitis [9]. To address the question whether presence of this cytokine in the eye during uveitis had a pathogenic or a protective role, we neutralized IL-22 by administering neutralizing antibody during the efferent phase of disease either systemically (five i/p injections starting on day 7 post immunization every other day) or locally just prior to clinical disease onset (intravitreal injection on day 8). Irrespective of whether IL-22 was neutralized systemically (Fig. 3A) or only locally in the eye (Fig. 3B), there was a significant increase in disease severity compared to the group that received isotype control. It should be noted that antibodies administered systemically would enter the eye once the blood-retinal barrier is breached during active disease. This suggested to us that IL-22 in the ocular tissue may have local effects that attenuate inflammation-induced tissue damage.

3.4. Retinal glial Muller cells express a functional IL-22 receptor and its expression is enhanced during EAU

We hypothesized that if local neutralization of IL-22 in the eye can have an effect on EAU severity (Fig. 3B) its receptor should be
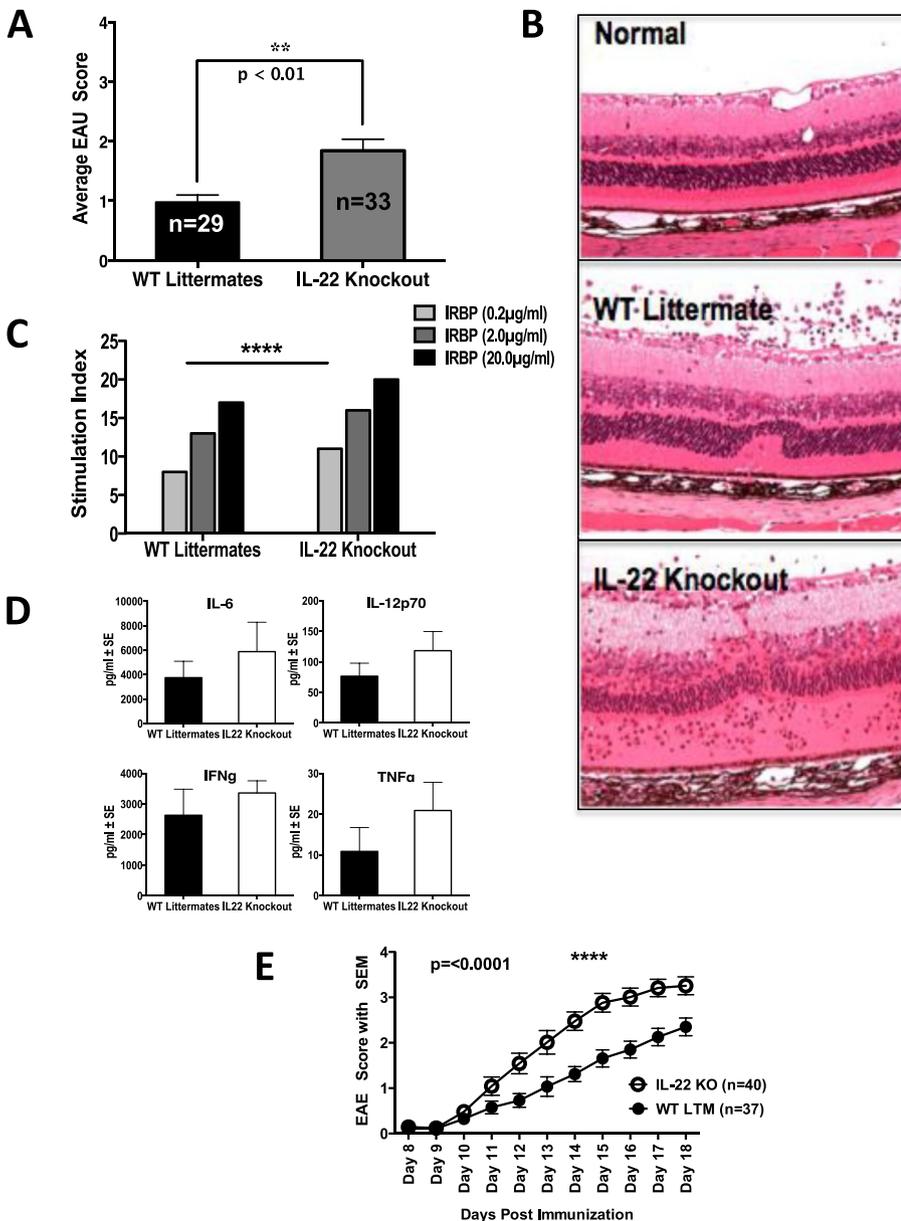
Fig. 2. Genetic deficiency of IL-22 results in more severe EAU and EAE. IL-22 knockout (KO) mice and their wild type littermates (WT LTM) were immunized with IRBP protein and human IRBP peptide 1–20. (A) Shown are average disease scores of both eyes of individual mice on day 21 p.i. from four separate experiments. Data were analyzed by Mann-Whitney *U* test (p = 0.002). (B) Histopathology of EAU eyes in IL-22 deficient (Knockout) and WT Littermate mice. Thickening of retinal layers and destruction of retinal architecture is more pronounced in the IL-22 knockout mice compared to their WT littermates. Original magnification of the image is ×200. (C–D) Antigen induced T cell memory response and cytokine production are enhanced in IL-22 knockout mice. (C) Lymphocytes from IL-22 KO mice showed significantly higher antigen specific memory immune response (lymphocyte proliferation assay with IRBP for 72 h) compared to that of WT Littermates. Shown is one of two independent experiments. Differences between groups were analyzed using 2-way ANOVA. (D) A non-significant increase in pro-inflammatory cytokines was observed in the IL-22 KO mice. Draining lymph node cells were cultured with 20 μg/ml IRBP for 48 h and culture supernatants were collected for multiplex cytokine assay (Bioplex) using the Luminex system (BioRad). Shown is data from one of two independent experiments. (E) IL-22 KO mice and their wild type littermates were immunized with MOG_{35-55} for inducing EAE and severity of disease was scored daily. Differences between strains were analyzed by two-way ANOVA. Shown are pooled data from three independent experiments.

expressed on ocular tissues. Expression of IL-22Rα1 had been reported in epithelial surfaces like skin, mucosal surfaces, respiratory tract, and endothelial surfaces of the blood brain barrier. In the human brain, IL-22Rα1 expression co-localized with astrocytes [25]. In the retina, there are few astrocytes compared to brain. The main macroglial cell population, characterized by expression of glial fibrillary acidic protein (GFAP), are the Müller cells. Enhanced expression of IL-22Rα1 was observed in the posterior segment of murine eyes following immunization with IRBP compared to a non-inflamed eye and their expression, which co-localized to cells expressing GFAP, followed a staining pattern reminiscent of Müller cells (Fig. 4A).

In order to examine effects of IL-22 on retinal glial Müller cells, we established primary Müller cell cultures from mouse retinas as previously described. When Müller cells were incubated with recombinant IL-22, their expression of IL-22Rα1 was enhanced (Fig. 4B), suggesting that IL-22 enhances expression of its own receptor on retinal glial cells through a positive feedback loop. A significant increase in expression levels of both IL-22Rα1 and GFAP (Fig. 4C) were noticed following rIL-

22 treatment *in vitro,* indicating activation of Müller cells through the Mapk/Stat3 pathway (Fig. 4D).

3.5. Treatment of Muller cells with IL-22 enhanced the suppression of T cell proliferation by Muller cells

An important function of Müller cell in the eye is functional and metabolic support of retinal neuronal health [26]. Our previous work suggested that in the context of inflammation, Muller cells may play an immunoregulatory protective role. They potently inhibit T cell activation and function *in vitro* [27] and, *in vivo*, incidence of uveitis is enhanced when Müller cells are damaged by a gliotoxic agent [28]. The findings in Fig. 4, showing expression of IL-22Rα1 is expressed on Müller cells, is enhanced during EAU, and is upregulated by IL-22 *in-vitro*, raised the possibility that the protective effects of IL-22 in the eye may be mediated, at least in part, by Müller cell inhibition of uveitogenic T cells. We therefore examined whether IL-22 can enhance the ability of Müller cells to inhibit T cell activation and proliferation.

A Systemic – Intraperitoneal injection
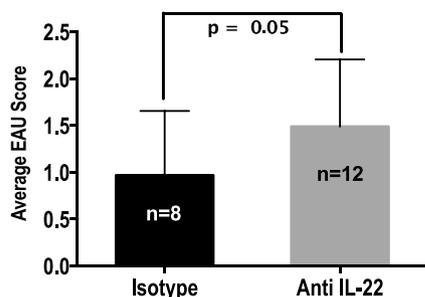
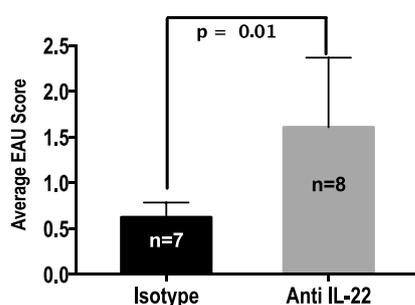## B Local – Intra vitreal injection

Fig. 3. Systemic and local neutralization of IL-22 levels during adaptive phase increases EAU severity. C57BL/6J mice were immunized with IRBP and were treated systemically or locally with IL-22 neutralizing antibody. (A) Mice treated systemically with anti-IL-22 neutralizing antibody had significantly higher disease than the controls. 500 μg of anti-mouse IL-22 (clone 8E11) or its isotype control antibodies were given intraperitoneally on days 7, 9, 11, 13, and 15 post-immunization. Data shown are average disease scores of individual mouse eyes on day 21. Results were pooled from two separate experiments and were analyzed by Mann-Whitney U method (p = 0.05). (B) Mice treated locally with anti-IL-22 neutralizing antibody had significantly higher disease than the controls. Each eye was injected intravitreally with either anti-mouse IL-22 or its isotype control antibodies (7 μg antibody in 2 μl/eye) on day 8 after uveitogenic immunization. Result from one out of three similar experiments is shown below. Data were analyzed by Mann-Whitney U method (p = 0.01).

Müller cells from primary cultures (up to 7 passages) were pre-treated, or not, with rIL-22 and were co-cultured with T cells in the presence of anti-CD3/CD28. IL-22 was able to enhance the inhibitory effect of primary Müller cells on T-cell proliferation (Fig. 5). Beyond 7 passages in culture, the ability of Müller cells to inhibit T cells, while still present, could no longer be regulated by IL-22.

3.6. Effect of IL-22 on retinal gene expression at the transcriptional level

To evaluate the functional effects of IL-22 in the eye during inflammation, we injected IL-1α with or without IL-22, into the vitreous cavity, isolated the retina and measured changes in expression of selected genes (Supplementary Table 1). The overall changes in the transcriptomic profile is shown as a heat map in Fig. 6A. Changes in the relative expression of some key mediators are shown in Fig. 6B. Compared to the expression profile of eyes injected with rIL-1α alone, retinas of eyes co-injected with IL-22 exhibited a relatively lower pro-inflammatory gene expression. This included Cxcl1, Cxcl2, Cxcl5, Ccl2, Tnf-α, Aldh1a2, Aldh1a3, Rara, Il12a, and Il23a, and MHC class II gene H-2A^b (Fig. 6B), which nevertheless were higher than in PBS injected

eyes. Even in the absence of an inflammatory stimulus, administration of recombinant IL-22 caused reduction in the transcript level of Cxcl5, a chemokine involved in neuroinflammation [29]. Conversely, co-injection of IL-22 with IL-1α enhanced the transcription of genes that are considered anti-inflammatory, e.g., Ccl11 (eotaxin-1), galectin genes Lgals1 and Lgals9, and the scavenger receptor Msr1 (Fig. 6B). Notably, administration of rIL-22 along with IL-1α increased the expression of IL-22 transcripts (Fig. 6A heat map) suggesting a positive feedback mechanism.

Analysis of gene expression data using pathway analysis tools is helpful to understand the significance of the results in a biological context. Fold change values from qRT-PCR data (Fig. 6) were imported into Ingenuity Pathway Analysis (IPA) tool for functional analysis of canonical pathways associated with these genes. Genes from our Taqman Array dataset were mapped onto the existing molecular networks in the knowledge base of IPA. We compared the gene expression profile of IL-1α injected retina with that of IL-1α + IL-22 injected retina using IPA's 'Core comparison' module. This analysis revealed several biological pathways that are altered by the treatment of IL-22 in an inflamed (IL-1α treated) retina. Selected pathways are shown in Fig. 6C. Presence of IL-22 inhibited expression of genes associated with T cell differentiation, apoptosis of ganglion cells, thymocyte cell death and antibody mediated cellular cytotoxicity (ADCC), whereas pathways leading to emigration of leukocytes and promotion of new DNA synthesis were enhanced. The overall change in the transcriptional network in the retinal tissue point towards pro-survival and anti-inflammatory effects that could help explain the observed neuronal sparing effects.

3.7. IL-22 enhances expression of neurotrophic factors in Muller cells

Since IL-22 receptor was detected only on retinal Muller cells (Fig. 4A) and since treatment of Muller cells with rIL-22 enhanced its expression (Fig. 4B and C) and activated Muller cells through phosphorylation of Stat3 (Fig. 4D), we tested whether IL-22 could trigger expression of neuroprotective factors that were previously reported to be produced by Muller cells in response to various other stimuli [30]. Compared to untreated Muller cells, IL-22 treated Muller cells produced significantly higher levels of Glial cell-derived neurotrophic factor (*Gdnf*), and Nerve growth factor (*Ngf*) (Table 1). In addition, IL-22-stimulated Müller cells had enhanced transcription of the anti-inflammatory genes Thrombospondin 2 (*Thbs2*) and *Il-19* (interleukin 10 family member). Expression of IL-10, assayed at the protein level, was not affected (data not shown). Taken together, our data suggest that IL-22 may act through Müller cells to protect the retina at 3 distinct levels: *(i)* by enhancing their contact-mediated suppression of autopathogenic T cells [27], *(ii)* by increasing their production of some anti-inflammatory mediators; and *(iii)* by stimulating Müller cells to express neurotrophic factors.

3.8. Presence of IL-22 protects retinal ganglion cells (RGCs) from glutamate induced neurotoxicity in vivo

Based on the results from Ingenuity pathway analysis tool (Fig. 6C) and the ability of IL-22-stimulated Müller cells to express neurotrophic factors, we hypothesized that IL-22 might play a neuroprotective role *in vivo*. To directly test this hypothesis, we induced neuronal toxicity by intraocular injection of glutamate in the presence or absence of IL-22. In this model, damage to neuronal cells is assessed as percent loss of RGCs as a result of glutamate toxicity. Our results show that mice genetically deficient in IL-22 experienced a significantly higher loss of RGCs compared to their WT littermates (Fig. 7A). Conversely, supplementation of endogenous IL-22 concurrently with intravitreal
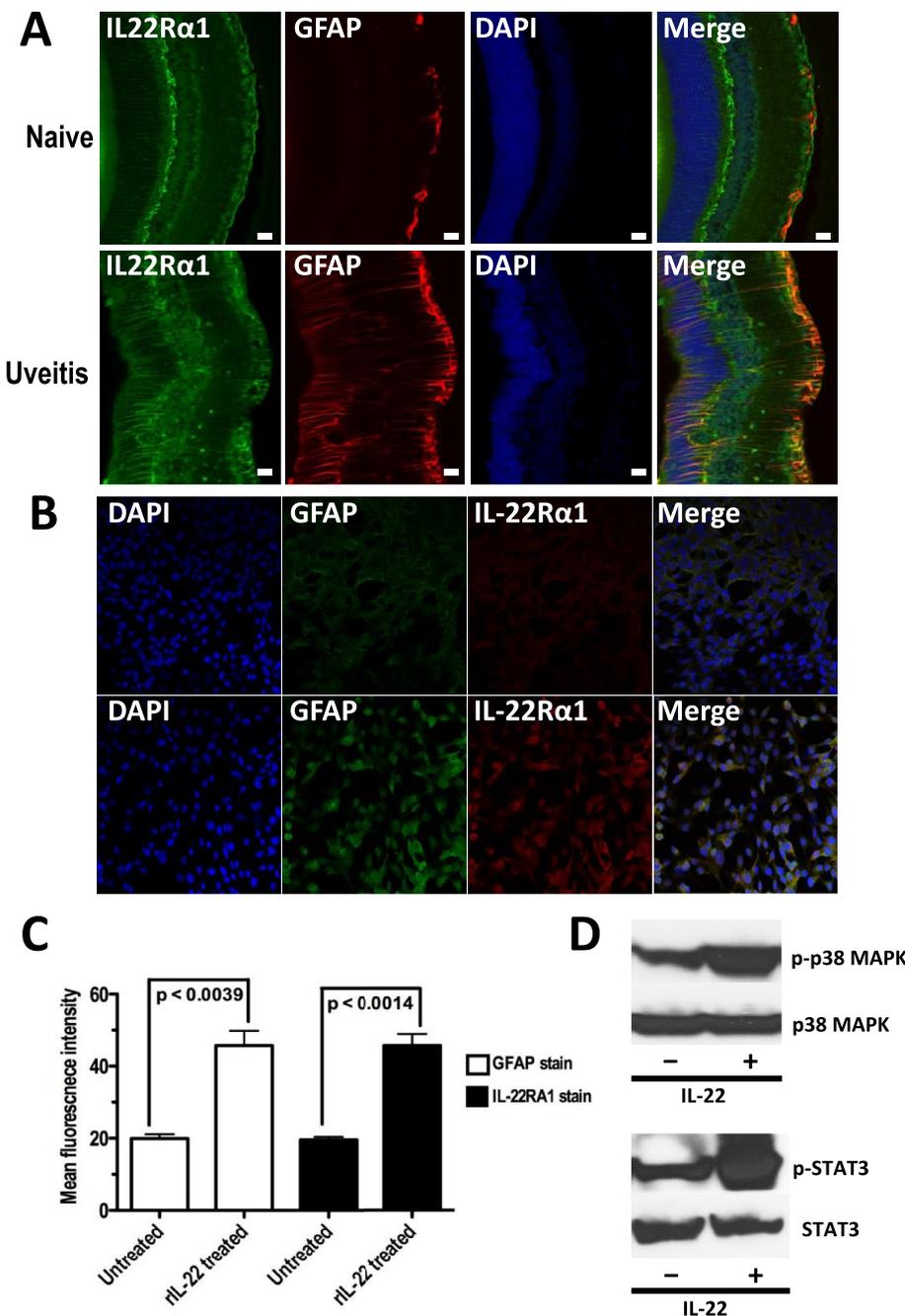
Fig. 4. Retinal Muller cells express IL-22Rα1 and respond to IL-22 stimulation by activating Stat3 and Mapk. (A) Retinal sections (thickness of 100 μm using Vibratome) of eyes from naïve and IRBP immunized (day 22) C57BL/6J mice were stained with anti-human IL-22Rα1 (green), anti-mouse GFAP (red), and DAPI. Images from naive eye and uveitic eye are shown. (B) Expression of IL-22Rα1 was enhanced when Muller cells in culture was treated invitro with rIL-22. Adherent Muller cells were stained with DAPI, anti-mouse GFAP (Alexa 488), and anti-human IL-22Rα1 (Alexa 555). Images from untreated Muller cells and rIL-22 treated (100 ng/ml for 24 h) Muller cells are shown. (C) Mean fluorescent intensity of GFAP and IL-22Rα1 staining in rIL-22 treated and untreated Muller cells show significantly high receptor expression within 24 h. p-value is calculated by two-tailed unpaired 't' test. (D) Phosphorylation of Stat3 and p38 subunit of Mapk was enhanced in Muller cells when treated with rIL-22 (500 ng/ml for 45 min) compared to that in untreated Muller cells.

glutamate administration, reduced the loss of RGCs due to glutamate intoxication (Fig. 7B). These data support a neuroprotective role for IL-22 in the CNS.

4. Discussion

IL-22 is a cytokine with multiple activities and its effects are complex and highly context-dependent [31]. On the one hand, IL-22 promotes antibacterial host defense and tissue remodeling, both involving induction of mediators that also have pro-inflammatory functions that may themselves be harmful to the tissue but may minimize microbial-induced damage. On the other hand, IL-22 has proliferative and anti-apoptotic effects by inducing pro-survival molecules including Bcl-2 and Bcl-xL as well as proliferation related molecules such as c-Myc and

Cyclin D1. IL-22 also enhances barrier function which contributes to its tissue protective effects. The net effect on the tissue will therefore depend on which of the processes predominate. Pro-inflammatory effects have been reported in animal models of rheumatoid arthritis, bleomycin-induced airway inflammation and psoriasis, whereas protective effects were seen in models of liver disease, intestinal and lung infection as well as hypersensitivity pneumonitis [32,33]. Importantly, the protective effects of IL-22 in the eye are not simply a recapitulation of the observations in gut, liver and lung. While in these tissues the protective effects can be largely attributed to enhanced mucosal barrier function, our data in the neuroretina point to direct or indirect anti-inflammatory and neuroprotective effects in the CNS.

Using the well-established model of EAU induced by immunization with the retinal autoantigen IRBP, we report that IL-22 has protective
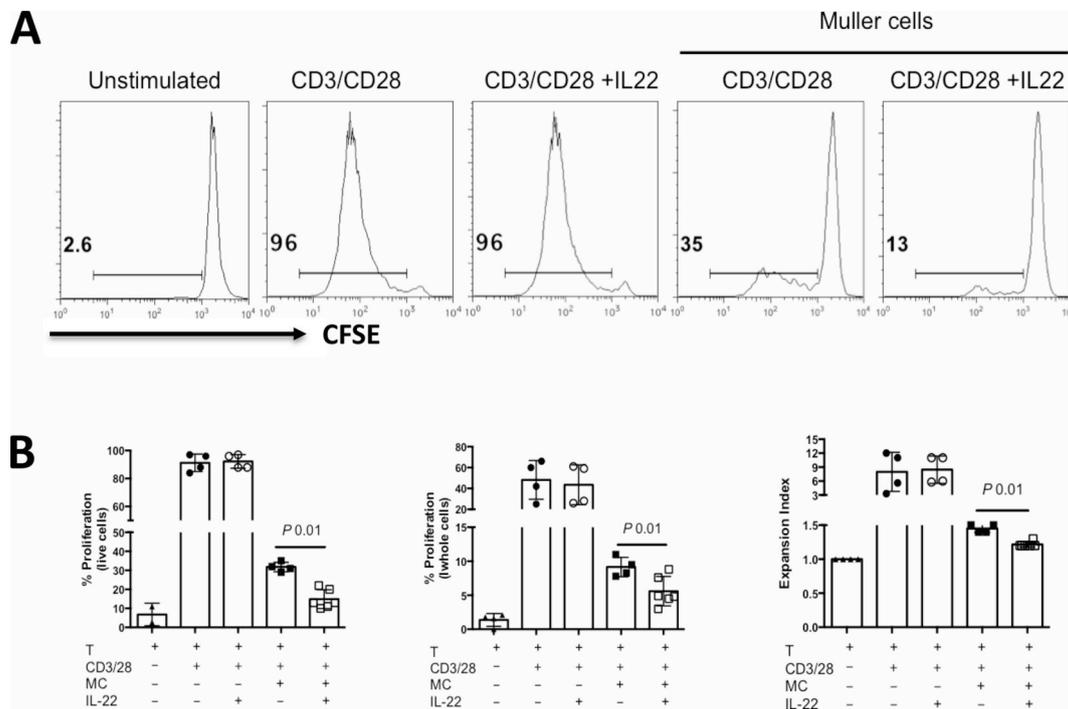
Fig. 5. Inhibition of T-cell proliferation is enhanced when Muller cells were pretreated with IL-22 *in-vitro* Murine T cells (enriched) were co-cultured with or without irradiated Muller cells previously isolated from naïve mice and cultured in-vitro (< 7 passages) in the presence or absence of 500 ng/ml rIL-22 for 72 h (A) Histogram showing dilution of proliferation dye eF670 in T cells stimulated with anti-CD3 and anti-CD28 for 72 h. Percentage of proliferating cells (live cell gate) is shown. (B) Bar graphs showing percentages of proliferating cells (of the data in panel A) among total live cell population, whole cell population, and the expansion index calculated by proliferation tool in FlowJo.

effects on the ocular tissue, as evidenced by the finding that neutralization of IL-22 in the ocular environment during the expression phase of disease, at a stage when autoaggressive lymphocytes have already been generated, resulted in more severe pathology. Of note, we found that IL-22-deficiency aggravated disease also in EAE, which shares with EAU many essential mechanisms that culminate in CNS neuropathology. Two previous studies examined effects of IL-22 in the EAE model: while one reported no effect of genetic IL-22 deficiency [23], another found that absence of IL-22 binding protein, which has the effect of increasing the amount of available IL-22, reduced EAE severity [24]. Our results, showing exacerbation of EAE in IL-22−/− mice, are in line with the latter, and support the conclusion that IL-22 has protective effects throughout the CNS.

Our data suggested that the protective action of IL-22 is mediated at least in part by local effects on the neuroretina, potentially involving retinal glial Müller cells, which express functional IL-22R and actively suppress activated T cells. Of interest, IL-22R expression has been reported in primary cultures of endothelial cells of the blood brain barrier (BBB) [34] as well as in brain lesions of multiple sclerosis patients, where it co-localized with astrocytes, a cell type that is closely related to retinal glial Müller cells [25]. To our knowledge, there are no data on IL-22R expression in retina of uveitis patients, or healthy subjects. In addition, our findings that IL-22 ameliorated glutamate-induced ganglion cell loss *in vivo* suggest existence of a neuroprotective effects on retinal neurons. We speculate that the neuroprotective effect of IL-22 on neurons would likely be indirect, as in contrast to Müller cells, our immunohistochemical stains did not reveal detectable expression of IL-22Rα on neuronal cells in the retina.

The ability of IL-22, co-injected into the eye together with IL-1, to modify the IL-1-induced inflammatory signature, can give mechanistic clues to the types of complex effects that may be at play. By Ingenuity pathway analysis, we noted inhibition of proinflammatory pathways (e.g., TNF-α, MHC class II, chemokines) and enhancement of anti-inflammatory pathways (e.g., galectins, macrophage scavenger receptors). Particularly provocative were effects compatible with enhanced DNA synthesis/repair and protection of ganglion cells from apoptosis, which are in line with the ability of IL-22-stimulated Müller cells to express neurotrophic factors *in vitro*, and is supported by *in vivo* data showing improved survival of RGC after glutamate challenge in IL-22 sufficient mice. Further in-depth dissection and follow up of these complex effects and their direct and indirect mediators await future studies.

Our data differ from a previous report, where the authors reported amelioration of EAU by systemic injections of recombinant IL-22 before disease onset. They concluded that IL-22 elicits tolerogenic dendritic cells that promote T-reg induction [12]. While our data do not exclude systemic effects of this type, in our hands, systemic treatment with recombinant IL-22 across a range of doses was not protective. The reason for this discrepancy is unknown. We speculate that this could be related to differences in commensal microbiome, as IL-22 affects intestinal barrier function and flora, and EAU development is affected by the microbiome [35,36].

In summary, our study adds a new dimension to what is known about the multi-faceted effects of IL-22, which vary with tissue and disease condition. From our data using mouse models of two CNS autoimmune diseases EAU and EAE, it appears that, IL-22 plays a tissue protective and possibly a regenerative role in the CNS. The neuroprotective effects are likely to combine multiple direct and indirect pathways involving ocular resident cells and their function, as well as the infiltrating inflammatory cells. Further study of the pathways regulated by IL-22 may enhance our understanding of neuroinflammation and instruct novel approaches to its modulation by augmenting natural neuroprotective mechanisms.
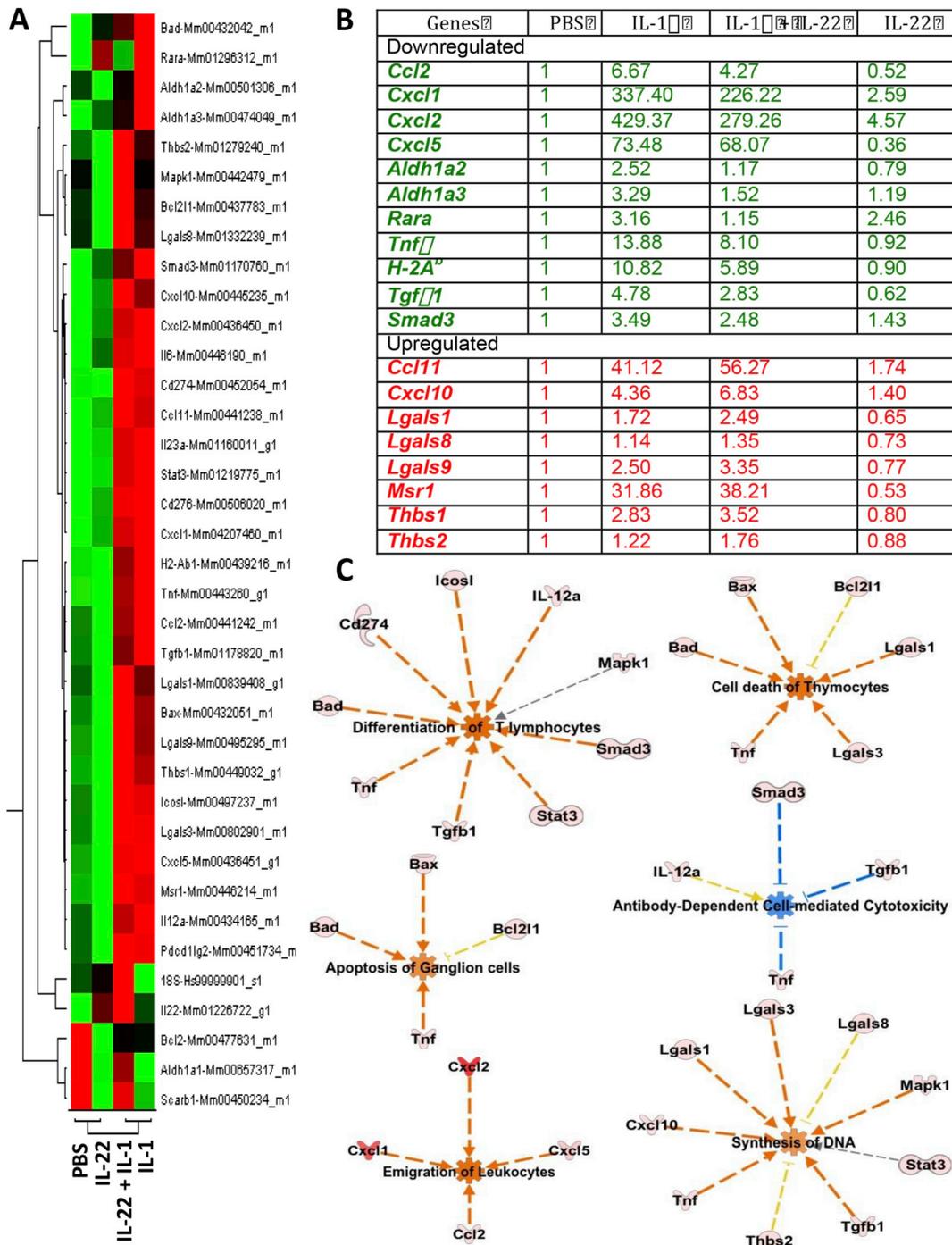
Fig. 6. IL-22 alters transcription profile of many genes during active inflammation in the eye. C57BL/6J mice were injected intravitreally with 2 μl of PBS, or 2 μl (100 ng) of recombinant IL-1, or 2 μl (200 ng) of recombinant IL-22, or a mixture of both IL-1α(100 ng) and IL-22 (200 ng) in a total volume of 2 μl, into each eye. Retinal tissues from 8 to 10 eyes/group were collected 24 h after injection and were pooled within each group for RNA isolation and real-time RT-PCR. Relative expressions of selected genes were compared after normalizing them to 'murine Gapdh' expression (endogenous control) and to PBS injected group (reference sample). Experiment was repeated twice and data (comparative CT) from two independent experiments were analyzed using 'Comparative CT study' in 7500 software v2.0.6. In this method, CT values for each individual gene from two independent experiments were averaged before applying normalization. (A) Gene expression profile of four treatment groups from Comparative CT study shown as a heat map. (B) Relative fold expression levels of selected genes. (C) Functional pathways perturbed by IL-22 during inflammation in the eye. Presence of IL-22 in the eye during inflammation negatively regulate pathways directed towards acute inflammation and tissue damage and positively regulate pathways directed towards dampening immune response or promoting tissue growth. Using Ingenuity Pathway Analysis (IPA) software, 'Core comparison analysis' of the Fold changes in gene expression was done between samples treated with (i)IL-1 alone vs. (ii) IL-1 + IL-22. Shown here are selected functional pathways that had statistically significant differences between the two samples, based on the expression profile of genes included in this study. Predicted activation (red) or inhibition (blue) of a biological function in either one of the two samples and their predicted relationship (red line – leads to activation, blue line – leads to inhibition, gray – effect not predicted, yellow – findings inconsistent with state of downstream molecules) based on knowledge base (IPA) are depicted.
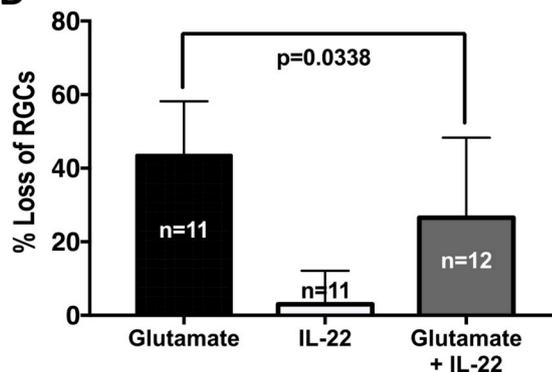
A
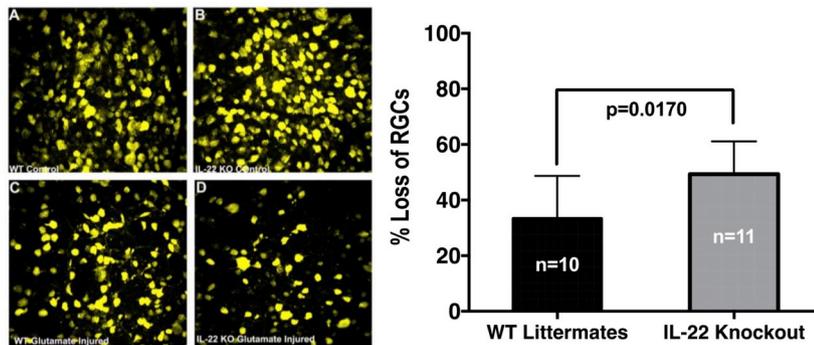
B

Fig. 7. Presence of IL-22 protects Retinal Ganglion Cells from glutamate induced neurotoxicity. C57BL/6J, IL-22 KO or its wild type littermates were subjected to retrograde labeling of RGCs with fluorogold followed by single intravitreal injection of glutamate with or without rIL-22. (A) Representative retinal flat mount images (40× magnification) from WT littermates or IL-22 KO mice with or without glutamate injury are shown. Histogram shows percentage loss of RGCs normalized to the contralateral control eyes from two independent experiments. IL-22 KO mice experienced significantly higher loss of RGCs when subject to glutamate injury. Data were analyzed by Welch's unpaired 't' test for significance. (B) Fluorogold labeled C57BL/6J mice were injected intravitreally with glutamate alone, rIL-22 alone or glutamate + rIL-22. Loss of RGCs in each group was normalized to a control group intravitreally injected with PBS. Data from two independent experiments were pooled and analyzed using one way ANOVA. Presence of IL-22 significantly decreased the loss of RGCs due to glutamate toxicity.

Appendix A. Supplementary data

Supplementary data to this article can be found online at https://doi.org/10.1016/j.jaut.2019.04.017.

References

[1] G.F. Sonnenberg, L.A. Fouser, D. Artis, Border patrol: regulation of immunity, inflammation and tissue homeostasis at barrier surfaces by IL-22, Nat. Immunol. 12 (2011) 383–390.
[2] L.A. Zenewicz, R.A. Flavell, Recent advances in IL-22 biology, Int. Immunol. 23 (2011) 159–163.
[3] K. Wolk, S. Kunz, E. Witte, M. Friedrich, K. Asadullah, R. Sabat, IL-22 increases the innate immunity of tissues, Immunity 21 (2004) 241–254.
[4] S. Aggarwal, M.H. Xie, M. Maruoka, J. Foster, A.L. Gurney, Acinar cells of the pancreas are a target of interleukin-22, J. Interferon Cytokine Res. 21 (2001) 1047–1053.
[5] D.C. Gritz, I.G. Wong, Incidence and prevalence of uveitis in Northern California; the Northern California epidemiology of uveitis study, Ophthalmology 111 (2004) 491–500 discussion.
[6] R.R. Caspi, A look at autoimmunity and inflammation in the eye, J. Clin. Investig. 120 (2010) 3073–3083.
[7] R. Horai, R.R. Caspi, Cytokines in autoimmune uveitis, J. Interferon Cytokine Res. 31 (2011) 733–744.
[8] D. Luger, P.B. Silver, J. Tang, D. Cua, Z. Chen, Y. Iwakura, et al., Either a Th17 or a Th1 effector response can drive autoimmunity: conditions of disease induction affect dominant effector category, J. Exp. Med. 205 (2008) 799–810.
[9] Z. Li, B. Liu, A. Maminishkis, S.P. Mahesh, S. Yeh, J. Lew, et al., Gene expression profiling in autoimmune noninfectious uveitis disease, J. Immunol. 181 (2008) 5147–5157.
[10] S. Sugita, Y. Kawazoe, A. Imai, T. Kawaguchi, S. Horie, H. Keino, et al., Role of IL-22- and TNF-alpha-producing Th22 cells in uveitis patients with Behcet's disease, J. Immunol. 190 (2013) 5799–5808.
[11] Y. Kim, T.W. Kim, Y.S. Park, E.M. Jeong, D.S. Lee, I.G. Kim, et al., The role of interleukin-22 and its receptor in the development and pathogenesis of experimental autoimmune uveitis, PLoS One 11 (2016) e0154904.
[12] Y. Ke, D. Sun, G. Jiang, H.J. Kaplan, H. Shao, IL-22-induced regulatory CD11b+ APCs suppress experimental autoimmune uveitis, J. Immunol. 187 (2011) 2130–2139.
[13] Y. Zheng, D.M. Danilenko, P. Valdez, I. Kasman, J. Eastham-Anderson, J. Wu, et al., Interleukin-22, a T(H)17 cytokine, mediates IL-23-induced dermal inflammation and acanthosis, Nature 445 (2007) 648–651.
[14] D.R. Pepperberg, T.L. Okajima, H. Ripps, G.J. Chader, B. Wiggert, Functional properties of interphotoreceptor retinoid-binding protein, Photochem. Photobiol. 54 (1991) 1057–1060.
[15] P.B. Silver, L.V. Rizzo, C.C. Chan, L.A. Donoso, B. Wiggert, R.R. Caspi, Identification of a major pathogenic epitope in the human IRBP molecule recognized by mice of the H-2r haplotype, Investig. Ophthalmol. Vis. Sci. 36 (1995) 946–954.
[16] R.R. Caspi, Experimental autoimmune uveoretinitis in the rat and mouse, Curr. Protoc. Im. (2003), https://doi.org/10.1002/0471142735.im1506s53 (Chapter 15):Unit 15 6.
[17] B. Becher, B.G. Durell, A.V. Miga, W.F. Hickey, R.J. Noelle, The clinical course of experimental autoimmune encephalomyelitis and inflammation is controlled by the expression of CD40 within the central nervous system, J. Exp. Med. 193 (2001) 967–974.
[18] F.G. Roberge, R.R. Caspi, C.C. Chan, T. Kuwabara, R.B. Nussenblatt, Long-term culture of Muller cells from adult rats in the presence of activated lymphocytes/monocytes products, Curr. Eye Res. 4 (1985) 975–982.
[19] B.S. Winkler, Glycolytic and oxidative metabolism in relation to retinal function, J.

Gen. Physiol. 77 (1981) 667–692.

[20] J.M. Skeie, S.H. Tsang, V.B. Mahajan, Evisceration of mouse vitreous and retina for proteomic analysis, J Vis Exp. 50 (2011), https://doi.org/10.3791/2795 pii: 2795.

[21] J.M. Coquet, S. Chakravarti, M.J. Smyth, D.I. Godfrey, Cutting edge: IL-21 is not essential for Th17 differentiation or experimental autoimmune encephalomyelitis, J. Immunol. 180 (2008) 7097–7101.

[22] R. Liu, Y. Bai, T.L. Vollmer, X.F. Bai, Y. Jee, Y.Y. Tang, et al., IL-21 receptor expression determines the temporal phases of experimental autoimmune encephalomyelitis, Exp. Neurol. 211 (2008) 14–24.

[23] K. Kreymborg, R. Etzensperger, L. Dumoutier, S. Haak, A. Rebollo, T. Buch, et al., IL-22 is expressed by Th17 cells in an IL-23-dependent fashion, but not required for the development of autoimmune encephalomyelitis, J. Immunol. 179 (2007) 8098–8104.

[24] H. Laaksonen, A.O. Guerreiro-Cacais, M.Z. Adzemovic, R. Parsa, M. Zeitelhofer, M. Jagodic, et al., The multiple sclerosis risk gene IL22RA2 contributes to a more severe murine autoimmune neuroinflammation, Genes Immun. 15 (7) (2014) 457–465, https://doi.org/10.1038/gene.2014.36.

[25] G. Perriard, A. Mathias, L. Enz, M. Canales, M. Schluep, M. Gentner, et al., Interleukin-22 is increased in multiple sclerosis patients and targets astrocytes, J. Neuroinflammation 12 (2015) 119.

[26] A. Bringmann, T. Pannicke, J. Grosche, M. Francke, P. Wiedemann, S.N. Skatchkov, et al., Muller cells in the healthy and diseased retina, Prog. Retin. Eye Res. 25 (2006) 397–424.

[27] R.R. Caspi, F.G. Roberge, R.B. Nussenblatt, Organ-resident, nonlymphoid cells suppress proliferation of autoimmune T-helper lymphocytes, Science 237 (1987) 1029–1032.

[28] C.C. Chan, F.G. Roberge, M. Ni, W. Zhang, R.B. Nussenblatt, Injury of Muller cells

[29] L.Y. Wang, Y.F. Tu, Y.C. Lin, C.C. Huang, CXCL5 signaling is a shared pathway of neuroinflammation and blood-brain barrier injury contributing to white matter injury in the immature brain, J. Neuroinflammation 13 (2016) 6.

[30] S. Fu, S. Dong, M. Zhu, D.M. Sherry, C. Wang, Z. You, et al., Muller Glia are a major cellular source of survival signals for retinal neurons in diabetes, Diabetes 64 (2015) 3554–3563.

[31] E. Nikoopour, S.M. Bellemore, B. Singh, IL-22, cell regeneration and autoimmunity, Cytokine 74 (2015) 35–42.

[32] P. Kumar, K. Rajasekaran, J.M. Palmer, M.S. Thakar, S. Malarkannan, IL-22: An evolutionary missing-link authenticating the role of the immune system in tissue regeneration, J. Cancer 4 (2013) 57–65.

[33] S. Sanjabi, L.A. Zenewicz, M. Kamanaka, R.A. Flavell, Anti-inflammatory and pro-inflammatory roles of TGF-beta, IL-10, and IL-22 in immunity and autoimmunity, Curr. Opin. Pharmacol. 9 (2009) 447–453.

[34] H. Kebir, K. Kreymborg, I. Ifergan, A. Dodelet-Devillers, R. Cayrol, M. Bernard, et al., Human TH17 lymphocytes promote blood-brain barrier disruption and central nervous system inflammation, Nat. Med. 13 (2007) 1173–1175.

[35] R. Horai, C.R. Zarate-Blades, P. Dillenburg-Pilla, J. Chen, J.L. Kielczewski, P.B. Silver, et al., Microbiota-dependent activation of an autoreactive T cell receptor provokes autoimmunity in an immunologically privileged site, Immunity 43 (2015) 343–353.

[36] Y.K. Nakamura, C. Metea, L. Karstens, M. Asquith, H. Gruner, C. Moscibrocki, et al., Gut microbial alterations associated with protection from autoimmune uveitis, Investig. Ophthalmol. Vis. Sci. 57 (2016) 3747–3758.